

## STUDY OF DIFFERENT SENSOR TYPES FOR HIGH RESOLUTION LINEAR CCD-IMAGERS

J VAN DER SPIEGEL\*, J SEVENHANS, A THEUWISSEN, J BOSIERS,  
I DEBUSSCHERE and G DECLERCK<sup>†</sup>

*ESAT Laboratories, Department of Electrical Engineering, Katholieke Universiteit Leuven, Kard Mercierlaan 94, B3030 Heverlee (Belgium)*

(Received July 4, 1984, accepted in revised form September 11, 1984)

### Abstract

A comparative experimental study of five different sensor types for high resolution CCD imagers will be presented. Three diode sensors with different doping profiles and two MOS sensors with a transparent poly-Si gate and indium-tin-oxide gate were incorporated in the same CCD structure. Both CVD SiO<sub>2</sub> and polyimide were used as the insulation layer between the light shield and the metallization layer. Detailed measurements have been done on the optical and electrical characteristics of the different sensor configurations. The results show the superiority of the single and double implanted diodes, with polyimide as the insulation layer.

---

### 1 Introduction

Since the invention of charge-coupled devices (CCD) in 1970, a lot of progress has been made in the field of solid-state imaging devices. Due to the enormous advances of semiconductor technology, the implementation of thousands of sensors in both line arrays and area arrays has become feasible [1 - 3]. This has created substantial interest and new possibilities in the field of surveillance and inspection, facsimile, terrestrial imaging and astronomical spectroscopy.

The continuous increase in the number of photosensors has been accompanied by an optimization of the structure of linear arrays. The first integrated silicon image sensor was a self-scanned photodiode array with a digital shift register for the addressing. This structure had the inherent disadvantage of poor noise characteristics due to the switching action of the MOS transistors (fixed pattern noise) and the large output capacitance.

---

\*Present address: Department of Electrical Engineering, University of Pennsylvania, 200 South 33rd Street, Philadelphia, PA 19104, U S A

<sup>†</sup>Senior Research Associate of the Belgian National Research Fund for Scientific Research

of the common output line. This disadvantage could be overcome by the charge-coupled devices in which the information is stored and transferred as analog charge packets and detected in a small output capacitance [4]. The main disadvantage of this device is associated with the CCD sensor itself, which consists basically of a MOS-capacitor covered with a semi-transparent poly-silicon electrode. Absorption and reflection in this multiple layer structure severely degrade the spectral response characteristics and the response uniformity of the sensor. Some years ago a new structure was introduced, which consists of a photodiode sensor and a CCD shift register [5 - 7]. These devices, which are often called charge-coupled photodiode devices (CCPD), have the low noise characteristics of the CCD array and the optical properties of the diode sensor. The optical and electrical characteristics combined with the high packing density make them attractive for linear high resolution cameras. Table 1 summarizes the characteristics of the self-scanned diode array, the CCD and the CCPD image arrays.

The purpose of this study is a further optimization of the optical and electrical characteristics of the sensor array. A detailed theoretical and experimental investigation of both the shift registers and the sensors was done. Photodiodes with three different profiles and two MOS sensors were fabricated. The idea is to fabricate the sensors using the fabrication steps of a standard CCD process, with minimal modifications. For example, the photodiodes will be made by using the same diffusion as for source and drain or by using buried channel implantation. The MOS sensors are covered with a poly-silicon electrode or an indium-tin-oxide (ITO) gate. The three photodiodes and the poly-silicon sensor were incorporated in the same bilinear buried channel CCD. The ITO sensor was implemented in a separate CCD with the same structure as the other CCDs. The experimental results of spectral response, response uniformity, modulation transfer function and dark current will be presented and discussed.

TABLE 1

Characteristics of the diode, CCD and CCPD arrays

Characteristics	Diode array	CCD (poly-gate)	CCPD
Output capacitance	large	small	small
Noise	fixed pattern noise high output noise	low	low
Spectral response	good and uniform	poor blue response reflections in top layers	good
Transfer inefficiency	no	low in buried channel	low

## 2 Design considerations description of the sensor types

Both photodiodes and MOS-capacitors have been employed as sensors in CCD imagers. A photodiode has, in general, a better spectral response

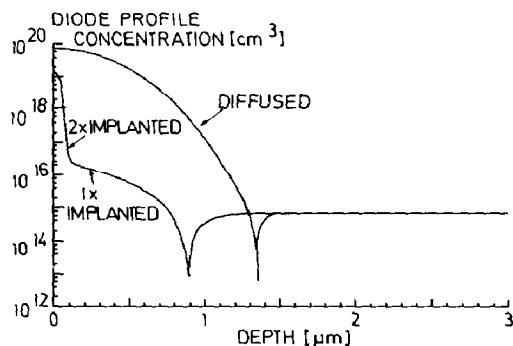


Fig 1 Diode profile of the three diode sensors

than an MOS sensor covered with poly-silicon. The photodiode with only a layer of silicon dioxide on top does not suffer so much from absorption and reflections. But the response of the diode is dependent on the diode doping profile, the junction depth and material parameters such as recombination lifetime, carrier mobility and surface generation. Chamberlain proposed a double implanted diode to improve the blue and visible wavelength quantum efficiency [8]. This type of diode, together with a single implanted and a diffused diode, has been incorporated in one CCD. Figure 1 gives the concentration profiles of the three diodes after a complete CCD process. The profiles were simulated by the program Supreme [9] and checked with spreading resistance measurements. The diffused diode has the highest surface concentration and the largest junction depth. The double implanted diode has the same profile as the single implanted one, except for the shallow arsenic implantation.

The MOS sensor covered with a semi-transparent electrode can be regarded as a field-induced junction, in which the collected electrons are stored in an inversion layer at the interface. The depletion layer extends from the surface on so that the minority carriers that are generated close to the surface will not recombine before they are collected. In this respect an MOS sensor is superior to the diode in which the generated carriers have to diffuse to the junction some distance away from the surface. On their way they might recombine, giving rise to a lower blue response. This inherent advantage of the MOS sensor can only be realized when the electrode is fully transparent. A poly-silicon electrode is not, especially in the blue region of the spectrum.

In order to take advantage of the MOS sensor, indium-tin-oxide, which has a high transmission in the visible spectrum, was implemented as an electrode [10]. This sensor will be compared with the four others.

### 3 Fabrication

Buried channel CCDs with three and four clock phases were built. The substrate is (100) p-type Si and has a resistivity of 24 - 26  $\Omega$  cm.

The charge-coupled devices were fabricated using a standard three layer poly-silicon technology. The gate oxide was grown in an oxygen atmosphere with 0.1% trichloroethane at 1025 °C, and had a thickness of 120 nm. The buried channel was implemented by a phosphorous implantation of  $1 \times 10^{12} \text{ cm}^{-2}$  or  $1.2 \times 10^{12} \text{ cm}^{-2}$  at 150 keV. The whole chip was covered by an aluminium shield in which a slit of 12  $\mu\text{m}$  was etched on top of the sensors. This aluminium layer was isolated from the bottom one by a 3  $\mu\text{m}$  CVD  $\text{SiO}_2$  or polyimide layer. The sensors were defined in the longitudinal direction by a 5  $\mu\text{m}$  wide stopper diffusion and thick oxide (locos). The sensor pitch was 12  $\mu\text{m}$ . The five sensor types were fabricated as follows:

(i) The diffused diode was realized by the phosphorous diffusion, which also defines the source and drain diodes.

(ii) The phosphorous implanted diodes were fabricated together with the channel implantation.

(iii) The double implanted photodiodes were made in two steps. The first implantation was the same as the buried channel implant. The second implantation was an additional arsenic implant of  $1.0 \times 10^{14} \text{ cm}^{-2}$  dose and 30 keV energy.

(iv) The fourth sensor type was an MOS capacitor covered with a poly-silicon electrode made in the third poly-silicon layer, which has a thickness of 500 nm. Because this poly-silicon layer was also used as electrode material in the shift registers, this thickness has not been optimized to achieve maximum quantum efficiency. This sensor was not implanted.

(v) The fifth sensor was covered with an indium-tin-oxide electrode. This sensor was incorporated in a separate CCD.

The indium-tin-oxide layer (ITO) was implemented after the first etching of the contact windows of the CCD shift registers, but before the final high temperature treatment. A d.c. magnetron sputtering technique was applied to deposit the ITO film on the wafers. The metal target (90% In-10% Sn) was sputtered in a reactive atmosphere (50%  $\text{O}_2$ -50% Ar) to give a transparent non-conductive ITO-film. After wet etching of the layer (positive resist, HI-etchant), the standard CCD process is continued. At the end of the complete process, including the final annealing step at 450 °C in forming gas, the ITO-strips which act as gates had the following characteristics:

thickness	400 nm
sheet resistance	10 $\Omega/\square$
light absorption	< 5% for $\lambda = 500 \text{ nm}$ < 30% for $\lambda = 400 \text{ nm}$
refractive index	2

The applied ITO-technology needs only one extra photo-mask and a few extra processing steps in comparison with the standard CCD process.

## 4 Results and discussion

### A Dark Current

The dark current, which is the result of thermal generation in a charge-coupled device, is one of the most important electrical characteristics. The thermally generated charges, which constitute the dark current, add to the optically generated carriers and distort the output signal. A detailed study was done on 250 CCDs. The average values of the dark signal after 1 s integration time are given in Table 2. Little difference was found between the first four sensor types. The contribution to the signal after 1 s is only 15% of the saturated output signal, and about 50% of the buried channel maximum output signal. The ITO-covered MOS sensor has a much larger dark current. This is due to the radiation damage introduced during the ITO sputtering. The dark current non-uniformity was found to be the same for all sensor types and was less than +4%.

In order to find out the main contribution to the dark current, the dark signal was measured as a function of the integration time by operating the CCD in the integration mode. Figure 2 depicts the result of the experiment for a double implanted diode. A similar response was observed for the other sensor types. Using an active area of  $2.9 \times 10^{-5} \text{ cm}^2$ , a dark current density of  $2.9 \text{ nA/cm}^2$  is found. The ITO sensor has a dark current density

TABLE 2

Average dark signal output after 1 s integration time at 22 °C

Sensor type	Diffused	1 × impl	2 × impl	Poly	ITO
$V_{\text{out}}$ (mV)	214	221	215	229	1100
Standard deviation (mV)	38	41	36	46	110

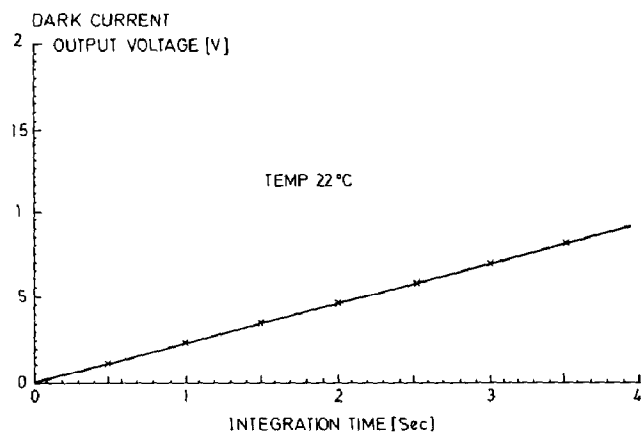


Fig 2 Dark signal output as a function of the integration time during CCD operation (temp 22 °C)

of  $15 \text{ nA/cm}^2$ . At room temperature the dark current in a CCD consists of the generation current  $J_g$  in the space charge layer and the surface generation current  $J_s$

$$J_g = qn_1W_G/\tau_g \quad (1)$$

$$J_s = qn_1s_0 \quad (2)$$

where  $q$  is the elementary charge,  $n_1$  the intrinsic carrier density,  $\tau_g$  the generation lifetime,  $s_0$  the surface generation current at a depleted surface and  $W_G$  the generation width [11]. The generation width decreases with the number of collected charges in a packet so that expression (1) will cause a non-linear dependence of the dark current on the integration time. This was not observed in the experiments, as illustrated in Fig. 2. The good uniformity of the dark current and its observed linear time dependence also rule out dislocations and other near surface defects as the main cause of the current [12]. This implies that the generation at the depleted surface is the main generation source. Pulsed capacitor measurements revealed a generation lifetime of 9 ms for the CCDs without the ITO layers. Using this value in eqn. (1) gives a generation current in the space charge layer of only  $0.07 \text{ nA/cm}^2$ , which confirms the former observation. By disconnecting the sensors from the CCD shift registers by proper biasing of the transfer and storage gate, it was found that the contribution of the sensor itself to the total dark current was less than 10%. Using expression (2) and an area of  $1.8 \times 10^{-5} \text{ cm}^2$  for the depleted surface in the CCD shift registers, values of  $1.9 \text{ cm/s}$  and  $9.5 \text{ cm/s}$  are found for the surface generation velocity  $s_0$  for the sensor without and with an ITO gate, respectively. This leads to the conclusion that the main contribution to the dark current comes from the surface generation in the shift registers.

### B Response non-uniformity

The response non-uniformity was measured on the five sensor types as a function of the wavelength by illuminating the CCDs through interference filters with a bandwidth of 10 nm. The response non-uniformity (RNU) is defined as follows

$$\text{RNU} = \frac{\Delta V_s}{V_s} \times 100 \quad (3)$$

where  $\Delta V_s$  is the peak-to-peak non-uniformity and  $V_s$  is half the maximum output voltage. The results of the experiments are given in Fig. 3. The curves are average values over the tested CCDs. The RNU increases at both high and low wavelengths, except for the ITO sensor which has a constant RNU at short wavelengths. The lowest RNU is obtained for the single implanted diode and the highest for the poly-silicon covered MOS sensor. There are two causes for the non-uniformity. The first one is the geometrical definition of the sensor by the aluminium shield. Etch irregularities modify the sensor area and degrade the RNU. This effect is the same for all sensor types and

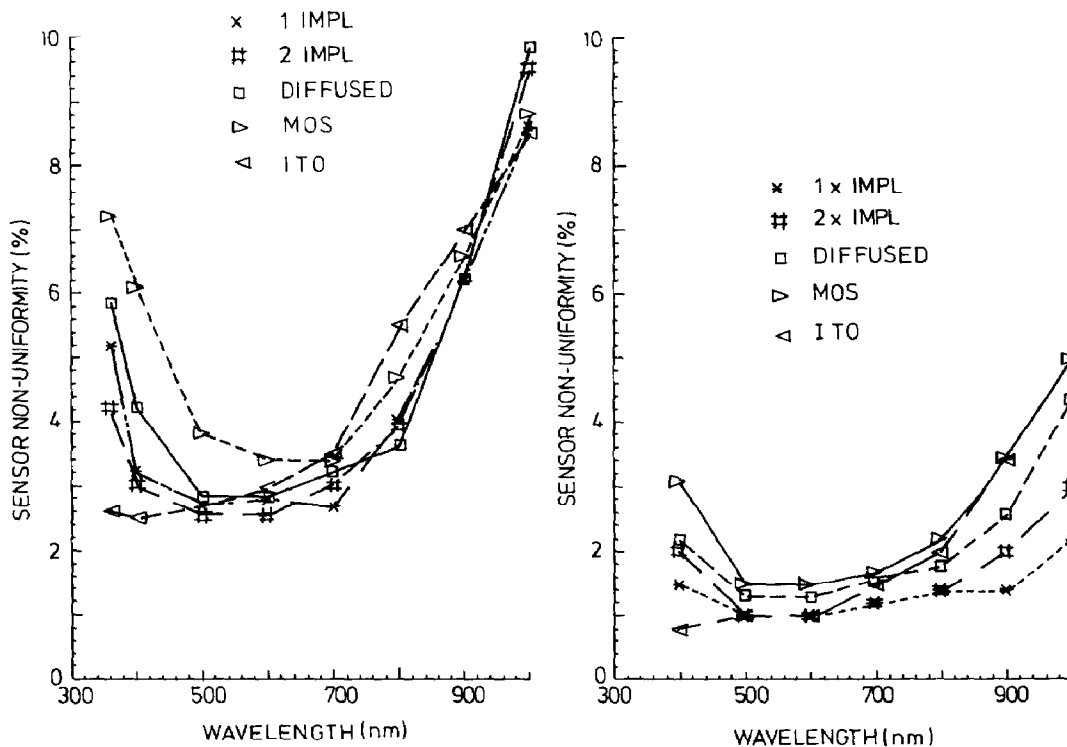


Fig 3 Response non-uniformity as a function of the wavelength for the sensors fabricated with CVD SiO<sub>2</sub> insulation

Fig 4 Response non-uniformity as a function of the wavelength for the sensors fabricated with a polyimide insulator

is wavelength independent. The smoother the surface, the better the slit in the aluminium can be defined. The influence of the etching was clearly demonstrated by replacing the CVD SiO<sub>2</sub> by polyimide as insulation. This gave rise to a much smoother surface and better etching of the aluminium layer [13]. The RNU measured on these devices is shown in Fig 4. A response non-uniformity as low as  $\pm 1\%$  can be obtained. The fact that the RNU is still wavelength dependent proves that another factor determines the uniformity. This component is due to variations in material, both on top of the sensor and in the bulk of the material, such as thickness non-uniformity and variations in surface and bulk recombination. At short wavelength irradiation, which has a small penetration depth, the surface properties are important. The thickness variation of the poly-silicon on top of the MOS sensor is particularly important and causes a significant non-uniformity. This explains the poor RNU of this sensor type. The indium-tin-oxide covered sensor, which has a much smaller absorption, suffers less from thickness variations. The single implanted diode has the lowest RNU, which stays quite constant up to 400 nm. The larger non-uniformity of the diffused and double implanted diode in this wavelength region might be due to the high surface concentration of phosphorous and arsenic respectively. As a

result of this, the surface region of the crystal will be more perturbed, which influences the surface recombination velocity and recombination lifetime. Also non-uniformities in the implantation can degrade the response uniformity.

The increase in RNU for wavelengths larger than about 750 nm is due to variations in the bulk generation. The average penetration depth is now considerably larger than the space charge layer width, so that the generated carriers have to diffuse before they are collected in the junction. Due to the bulk defects, the diffusion length will vary from place to place, influencing the number of collected carriers.

In the range between 500 nm and 700 nm the penetration depth of the light lies between 1  $\mu\text{m}$  and 2  $\mu\text{m}$ , so that most of the light is absorbed in the space charge layer, in which the recombination is negligible. This is the reason for the low RNU values in this spectral range.

The contributions to the RNU at 400 nm, in addition to the geometric one, are similar for both the CVD  $\text{SiO}_2$  and polyimide samples, except in the case of the MOS sensor. At a wavelength of 1000 nm, the difference in the additional RNU contributions between the  $\text{SiO}_2$  and polyimide samples is more pronounced for all sensor types. There is no clear reason why this difference would be caused by the presence of polyimide or  $\text{SiO}_2$ .

### C Spectral response and quantum efficiency

The spectral response  $R$  and the quantum efficiency were obtained from measurements of the output voltage at the on-chip pre-amplifier. The relationship between the output voltage  $V_o$ , the quantum efficiency  $\eta$  and the spectral response is as follows:

$$\eta = \frac{hc}{\lambda} \frac{V_o C_o}{\alpha_v} \frac{1}{q I_0 A_S T_{\text{int}}} \quad (4)$$

$$R = \frac{\lambda q \eta}{hc} \quad (5)$$

where  $q$  is the elementary charge,  $h$  is Planck's constant,  $c$  is the velocity of light,  $\lambda$  is the wavelength of the incident radiation,  $V_o$  is the output voltage,  $C_o$  is the output capacitance of the CCD,  $\alpha_v$  is the gain of the output amplifier,  $A_S$  the sensor area,  $T_{\text{int}}$  the integration time and  $I_0$  the incident light power density.

Figure 5 gives the spectral response of the five sensor types. On the same figure, the lines of constant quantum efficiency are also drawn.

The ITO sensor is superior to all other sensor types, especially in the blue region of the spectrum. With respect to the poly-silicon sensor, for wavelengths smaller than 600 nm the response of the ITO sensor is spectacular. This is due to the fact that the poly-Si storage gate absorbs a large amount of the incident light. If the wavelength of the light exceeds 600 nm, the difference in quantum efficiencies between the two capacitor sensors is still a factor 2.5. In this range of the visible spectrum, the poly-Si absorbs less incident

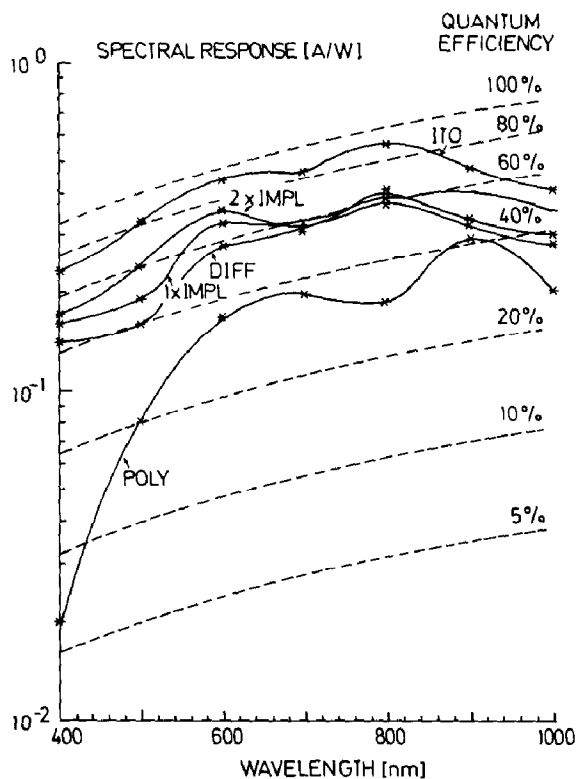


Fig 5 Spectral response and quantum efficiency of the five sensor types

photons and the residual gain in spectral response of the ITO sensor is mainly due to less reflective losses at the different interfaces of the structure. The higher response of the ITO sensor with respect to the different photodiodes is due to the better reflective characteristics of the structure with the ITO storage gate. The multi-layer structure can more easily be optically matched to the Si substrate than the single SiO<sub>2</sub> film of the photodiodes. Also the lack of high doping effects and the negligible surface recombination in the MOS sensors enhance their response compared with the photodiodes. In particular, the diffused photodiode suffers severely from high doping effects. As a result of this, the minority carrier lifetime decreases considerably, so that a substantial number of charge carriers recombine before they are collected in the junction. It has been proved by Chamberlain *et al* [14] that the previous phenomenon and the retarding field of the effective doping profile are the main causes of the response degradation in the blue spectral region. The implanted diodes, which have a lower doping level and a shallower junction, are much less influenced by the detrimental high doping effects. The built-in electric field in the double implanted diode is the reason why the profiled structure has a better response than the single implanted one.

### E Modulation transfer function (MTF)

The modulation transfer function was measured by projecting a black and white bar pattern upon the CCD through a high quality lens. In order to obtain the MTF, the measured square wave response must be transformed to a sine wave response. The MTF of the sensor is obtained by taking into account the MTF of the lens.

To compare the different sensor types, it is sufficient to take the square wave response. Figure 6 gives the results of the measurements for wavelengths of 500 nm and 800 nm. There is no pronounced difference between the sensor types, although the implanted diode has a slightly better MTF at 500 nm whereas the diffused diode with its larger junction depth is better at long wavelengths. The poly-silicon covered MOS sensor has the poorest MTF at both short and long wavelengths. For shorter wavelengths, this is caused by the thickness variation in the top layers. At longer wavelengths, the smaller MTF is due to the shallower space charge layer in comparison with the diodes.

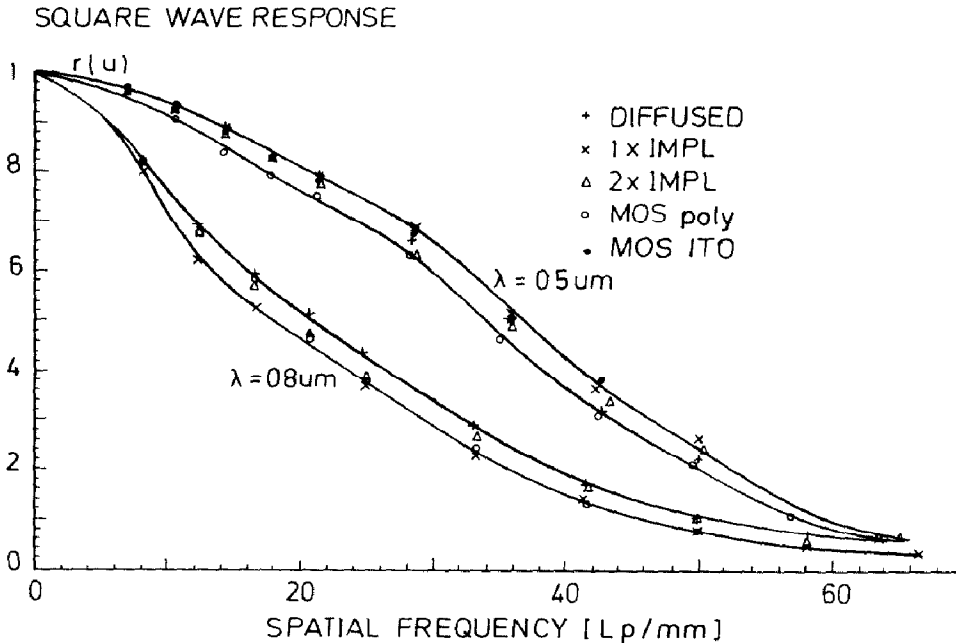


Fig 6 Square wave response of the system 'lens + sensor' as a function of spatial frequency at 500 nm and 800 nm

## 5 Conclusions

Five different sensor types, of which four were fully compatible with standard CCD technology, were implemented on the same CCD structure. The five sensor types were evaluated as far as dark current, response uniformity, spectral response and modulation transfer function are concerned.

TABLE 3  
Ranking of the five sensor types

Characteristics	Diode sensors			MOS Sensors	
	Diffused	1 × impl	2 × impl	Poly-Si	ITO
Dark current	(1)	(1)	(1)	(1)	5
RNU	4	1	3	5	2
Spectral resp	4	3	2	5	1
MTF, short $\lambda$	4	1	2	5	3
MTF, long $\lambda$	1	4	3	5	2

Table 3 gives an overview of the experiments performed and a ranking of the sensor types. The sensor with the best characteristics gets a "1", the one with the poorest a "5". When no considerable difference is found, the numbers are put in parentheses.

The dark currents for the diode and the poly-Si sensor were similar and very low. The ITO sensor had a much higher dark current, which was attributed to the radiation damage during sputtering of the ITO layer. The main contribution to the dark current in all the sensor types was the surface generation at the depleted surfaces in the shift registers. The response uniformity was found to be wavelength dependent and to increase at both long and short wavelengths. The geometrical influence of the non-uniformity was reduced considerably by using polyimide as insulation between the first metal layer and the aluminium light shield. The best results were obtained for the single implanted photodiode. The RNU for this sensor type was as good as  $\pm 1\%$ . For spectral response the ITO sensor was superior, especially in the blue region of the spectrum. The disadvantage of this sensor is that its fabrication technique has a detrimental influence on the dark current. High quantum efficiencies were also obtained with the double implanted diode, in which the built-in field helps the generated carriers to drift towards the junction. The modulation transfer function was obtained from the square wave response measurements. The five sensor types showed a similar behaviour. At short wavelengths the implanted diodes showed a slightly better MTF, whereas at long wavelengths the diffused diode is best because of the deeper junction. It can be concluded that the ITO sensor has superior optical characteristics but that because of the high dark current and the non-standard technology, it is less suited for CCD imagers. The ITO sensor is followed by the implanted diode. The double implanted one has better spectral response but the single implanted one has the best response uniformity. An argument in favour of the latter diode is its simple fabrication technology. The poorest results are obtained for the poly-silicon covered MOS sensor, and this is almost entirely due to the large absorption in the poly-silicon layer. This effect can be reduced by working with a thinner poly-silicon layer. The use of polyimide as isolation between the

two aluminium layers gives a pronounced improvement in response uniformity over CVD silicon dioxide

### Acknowledgements

The authors are grateful to V Muls and T Hendrickx who processed the devices and to T van Nuland and J Stevens who assisted with the measurements Part of the work was sponsored by the European Space Agency, under contract number ESTEC 4537/81/NL/PP

### References

- 1 T Yamada *et al*, A 3648 element CCD linear image sensor, *Techn Digest IEDM, Washington, Dec, 1982*, pp 320 - 323
- 2 L Sheu *et al*, 3533 Element quadrilinear CCD imager, *Techn Digest ISSCC, New York, Feb, 1983*, pp 252 - 253
- 3 M Blake *et al*, A 640 kilopixel CCD imager for space applications, *Techn Digest IEDM, Washington, Nov, 1978*, pp 412 - 414
- 4 M Tompsett *et al*, Charge-coupled imaging devices experimental results, *IEEE Trans Electron Dev, ED 18 (1972) 992 - 996*
- 5 J White and S Chamberlain, A multiple-gate CCD photodiode sensor element for imaging arrays, *IEEE Trans Electron Dev, ED 25 (1978) 125 - 131*
- 6 H Tseng and S Weckler, CCPD — the optimum solid state line scanner, in Y Brault (ed), *AGARD Conf Proc No 230*, pp 4 3 1 - 4 3 12
- 7 S Ohba *et al*, A 1024 element linear CCD sensor with a new photodiode structure, *IEEE Trans Electron Dev, ED-27 (1980) 1804 - 1808*
- 8 S Chamberlain, Profiled silicon photodetector for improved blue color and visible wavelength quantum efficiency, *Techn Digest IEDM, Washington, Dec, 1979*, pp 137 - 140
- 9 D Antoniadis, S Hauser and R Dutton, SUPREME II, a program for IC process modelling and simulation, *Techn report No 5019 2, Stanford University, 1978*
- 10 A Theuwissen and G Declerck, ITO technology for CCD imagers, *10th Essderc/5th SSSDT, York, 1980*, pp 216 - 217
- 11 J Van der Spiegel and G Declerck, Theoretical and practical investigation of thermal generation in gate-controlled diodes, *Solid State Electronics, 24 (1981) 869 - 877*
- 12 J Van der Spiegel and G Declerck, Characterization of dark current non-uniformities in charge-coupled devices, *Solid State Electronics, 27 (1984) 147 - 154*
- 13 A Theuwissen and G Declerck, Linear CCD imagers with a polyimide insulation for double level metallisation, *IEEE Electron Dev Letters, EDL 3 (1982) 308 - 309*
- 14 S Chamberlain *et al*, Spectral response limitation mechanisms of a shallow junction n+ -p photodiode, *IEEE Trans Electron Dev, ED 25 (1978) 241 - 246*

### Biographies

*Jan Van der Spiegel* was born on April 12, 1951, in Aalst, Belgium He received his M S and Ph.D degrees in electrical engineering from the Catholic University of Leuven in 1974 and 1979, respectively

From 1974 until 1979 he worked at the ESAT Laboratory of the University of Leuven on high resolution linear CCD image sensors and on the

characterization of thermal generation sources in CCDs. Since 1980, he has been with the Moore School of Electrical Engineering at the University of Pennsylvania. In 1981 he became Assistant Professor of Electrical Engineering. His main interests are in the area of integrated chemical, tactile and image sensors, and also in fast radiative processing of materials. In 1983 he received an IBM Young Faculty Development Award and in 1984 a Presidential Young Investigator Award.

Dr Van der Spiegel is a member of the IEEE, the Electrochemical Society and the Materials Research Society

*Jan Sevenhans* received his Ph D degree in electrical engineering from the Catholic University of Leuven in 1983

From October 1979 until February 1983 he was with the ESAT Laboratory of the University of Leuven, working on the development of a high resolution CCD line imager for facsimile applications. Since March 1983 he has been working with the E B S Department of Agfa-Gevaert N V

Dr Sevenhans is a member of the IEEE

*Albert Theuwissen* received his M S and Ph D degrees in electrical engineering from the Catholic University of Leuven in 1978 and 1983, respectively

From 1977 to 1983 he was with the ESAT Laboratory of the Leuven University where he worked on indium tin oxides and polyimides for CCD image sensors. In 1983 he joined the Philips Research Laboratories in Eindhoven where he is involved in the development of high resolution CCD TV cameras

Dr Theuwissen is a member of the IEEE

*Jan Bosiers* received his M S degree in electrical engineering at the Catholic University of Leuven in 1980

He has been working at the ESAT Laboratory of the University of Leuven on the development of a high resolution CCD line imager for facsimile applications. Since 1983, he has also been working on amorphous silicon contact imagers

Mr Bosiers is a member of the IEEE

*Ingrid Debusschere* received her M S degree in electrical engineering from the Catholic University of Leuven in 1981

Since September 1981 she has been with the ESAT Laboratory of the University of Leuven working towards Ph D degree. Her interests are in the area of X-ray sensitive CCD imagers and radiation hard CCD technologies

Mrs Debusschere is a member of the IEEE

*Gilbert Declerck* was born in Oostende, Belgium on October 21, 1946. He received his Ph D degree in electrical engineering from the University of Leuven in 1972

From 1973 to 1974 he was at the IC Laboratories of Stanford University. He joined the ESAT Laboratory of the Leuven University in 1974 where he is Professor and Senior Research Associate of the Belgian National Fund for Scientific Research. He is responsible for the CCD Technology and Applications Group, where the main interest is high resolution and special purpose image sensors. He is also involved in the development of advanced CMOS processes, in silicon crystal defects and in dry etching and optical and e-beam lithography for micrometer and submicrometer structures.

Dr Declerck is a member of the IEEE and the Electrochemical Society.